Electronic Supplementary Material (ESI)

A mesoporous C,N-co doped Co-based phosphate ultrathin nanosheet derived from phosphonate-based-MOF as an efficient electrocatalyst for water oxidation

Zhao-Qian Huang, Wen-Xiu Lu, Bin Wang, Wei-Jun Chen, Jie-Ling Xie, Dong-Sheng Pan, Ling-Li Zhou and Jun-Ling Song*

Table S1 Comparison of the OER catalytic performance of the other recently reported MOFs derived electrocatalysts supported on glass carbon in different media.

Catalyst	Substrate	Electrolyte	Overpotential at 10/-10 mA/cm^2 (mV vs.RHE)	Tafel slope (mV dec^{-1})	Reference
CoNi-P-3DHFLMs	GC	1 M KOH	292	84	*Applied Catalysis B: Environmental* **2019**, *249*, 147
Co_3O_4/MoS_2	NF	1 M KOH	230 (*j*=20 mA/cm^2)	94	*Applied Catalysis B: Environmental* **2019**, *248*, 202
			205	128	
FeNi@N-CNT	GC	1 M KOH	300	47.7	*ACS Appl. Mater. Interfaces* **2016**, *8*, 35390
S-CoWP@(S,N)-C	GC	1 M KOH	420	68	*ACS Energy Lett*. **2018**, *3*, 1434
			-67	35	
$(Co,Ni)Se_2$@NiFe LDH	GC	0.1 M KOH	277	75	*ACS Appl. Mater. Interfaces* **2019**, *11*, 8106
Ni_2P-CoP	GC	0.1 M KOH	320	69	*ACS Appl. Mater. Interfaces* **2017**, *9*, 23222
		0.5 M H_2SO_4	105	64	
Co-N-C NN-800	GC	0.1 M KOH	470	191	*ACS Appl. Energy Mater*. **2018**, *1*, 1060
$(Ni_{0.62}Fe_{0.38})_2P$	GC	1 M KOH	290	44	*Catal. Sci. Technol*., **2017**, *7*, 1549
CeO_x/CoS@L-CeO_2NRs	GC	1 M KOH	238	42	*J. Mater. Chem. A*, **2019**, *7*, 8284
$Co_3O_4/CoMoO_4$-50	GC	1 M KOH	318	63	*J. Mater. Chem. A*, **2018**, *6*, 1639
Mn-CoP	GC	1 M KOH	356	76	*Dalton Trans*., **2018**, *47*, 14679
		1 M KOH	195	85	
FeCo-P/C	GC	1 M KOH	362	50.1	*Small Methods* **2018**, *2*, 1800214
NGO/Ni_7S_6	GC	0.1 M KOH	380	45	*Adv. Funct. Mater.* **2017**, *27*, 1700451
			370	145.5	
Co_9S_8@TDC-900	GC	1 M KOH	330	86	*J. Mater. Chem. A*, **2019**, *7*, 7389
Fe_3C@NCNT/NPC	GC	1 M KOH	369	62	*Catal. Sci. Technol*., **2016**, *6*, 6365
Co_3O_4@C-MWCNTs	GC	1 M KOH	320	62	*J. Mater. Chem. A*, **2015**, *3*, 17392
Co/Co_9S_8@NSOC-800	GC	1 M KOH	373	80	*Chem. Commun.,* **2019**, *55*, 3203
			216	/	
Co_3O_4@Co/NCNT	GC	0.1 M KOH	380	58.7	*Chem. Eur. J*. **2017**, *23*, 18049
ZnCoNC-0.1	GC	0.1 M KOH	520	129	*Nano Res.* **2018***, 11(1):* 163
Co_9S_8@CT-800	GC	0.1 M KOH	390	72	*J. Mater. Chem. A*, **2018**, *6*, 5935

Co_4Ni_1P NTs	GC	1 M KOH	245	61	*Adv. Funct. Mater.* **2017**, *27*,
			129	52	1703455
Co/Ni@C	GC	0.1 M KOH	440	93	*ACS Appl. Energy Mater*. **2019**, *2*, 1854
CoP_3 CPs/CFP	GC	1 M KOH	343	76	*Phys. Chem. Chem. Phys.,* **2017**, *19*,
		0.5 M H_2SO_4	-78	53	2104
Co_9S_8/NSCNFs-850	GC	1 M KOH	302	54	*Small* **2018**, *14*, 1704035
CoO_x-MoC/NC-2	GC	1 M KOH	330	89	*Small* **2017**, *13*, 1702753
H3LCoCN800	GC	1 M KOH	267	64	*ACS Catal*. **2017**, *7*, 6000
	NF		215	61	
ZIF-8-C6	GC	0.1 M KOH	476	78.5	*Mater. Chem. Front.,* **2018**, *2*, 102
		0.5 M H_2SO_4	155	54.7	
porous Ni_2P	GC	1 M KOH	320	165	*J. Mater. Chem. A*, **2018**, *6*, 18720
			168	63	
$Co_2P/Mo_2C/Mo_3Co_3C$@C	GC	1 M KOH	362	82	*J. Mater. Chem. A*, **2018**, *6*, 5789
			182	68	
$(Ni,Co)Se_2$	GC	1 M KOH	256	74	*Nanoscale*, **2019**, *11*, 6401
Ni@NC-800	GC	1 M KOH	280	45	*Adv. Mater.* **2017**, *29*, 1605957
			205	160	
Co-NC/CNT	GC	1 M KOH	354	78	*J. Mater. Chem. A*, **2016**, *4*, 16057
			203	125	
14.6 % CeO_x/CoS	GC	1 M KOH	269	50	*Angew. Chem. Int. Ed*. **2018**, *57*, 8654
$CoSe_2$-450	GC	1 M KOH	330	79	*J. Mater. Chem. A*, **2017**, *5*, 15310
C-MOF-C2-900	GC	0.1 M KOH	350	79	*Adv. Mater.* **2018**, *30*, 1705431
Py-1@SNC600	GC	1 M KOH	284.7	56	*Small* **2019**, *15*, 1900348
Co–CNT/PC	GC	0.1 M KOH	315	73.8	*Chem. Commun.,* **2016**, *52*, 9727
$CoSe_2$/CFC	GC	1 M KOH	356	88	*ACS Appl. Mater. Interfaces* **2016**, *8*, 26902
CoNC-CNF-1000	GC	0.1 M KOH	450	94	*Small* **2018**, *14*, 1800423
NiCoS/$Ti_3C_2T_x$	GC	1 M KOH	365	58.2	*ACS Appl. Mater. Interfaces* **2018**, *10*, 22311
FeNi@NCNT	GC	1 M KOH	300	48	*ACS Appl Mater Interfaces*, **2016**, *8*: 35390
2D Co_3O_4/CBDC	GC	1 M KOH	208	50	*ACS Energy Lett*, **2018**, *3*: 1655
CoMo–H	GC	1 M KOH	312	69	*Adv Funct Mater*, **2017**, *27*: 1702324
NF@NC-$CoFe_2O_4$/C NRAs	GC	1 M KOH	240	45	*Adv Mater*, **2017**, *29*: 1604437
$CoSe_2$-450	GC	1 M KOH	330	79	*J Mater Chem A*, **2017**, *5*: 15310
$CoTe_2$@NCNTFs	GC	1 M KOH	330	83	*J Mater Chem A*, **2018**, *6*: 3684
CoP/rGO-400	GC	1 M KOH	340	66	*Chem Sci*, **2016**, *7*: 1690
NiCoP/C nanoboxes	GC	1 M KOH	330	96	*Angew Chem Int Ed*, **2017**, *56*: 3897

Experimental Section

Calculation Method: Details concerning the calculation of the Faraday efficiency for OER are shown below.

The turnover frequency (TOF) of the catalyst for OER is defined as

$$TOF = n_{O_2}/n_{cat}/t \quad (S1)$$

where n_{O_2} is the amount of oxygen (mol) produced, n_{cat} is the amount of catalytic active centers in the catalyst (mol) and t is the electrolysis time (s).

When the electrolysis current is all used for OER,

$$TOF_{theoretical} = J/(4\times F\times m/M) \quad (S2)$$

Where J is the current density (mA cm^{-2}) at a given overpotential, F is the faraday constant (96485 C mol^{-1}), m is the mass loading of the catalyst (mg cm^{-2}), and M is the molecular weight of the catalyst unified with one active center per formula unit.

The Faraday efficiency for OER is calculated by

$$F_{OER} = TOF / TOF_{theoretical} \times 100\% \quad (S3)$$

The obtained gas chromatography peak areas of O_2 and N_2 in the electrolytic cell are:

	0 min	10 min	20 min	40 min	60 min
O_2	2968.935	3065.909	3162.846	3357.463	3542.295
N_2	13109.658	12895.355	12352.472	11948.066	11096.842

Giving n_{O_2} = O_2 concentration (%) × head space volume / (22.4 × 298 / 273) = 573.36 / 13415.4 × 50 / 1000 / 24.45 mol = 8.74 × 10^{-5} mol. Because n_{cat} = mass loading (mg) / molecular weight / 1000 = 3 × 0.03 / 451.67 / 1000 =1.99 × 10^{-7} mol, TOF = 8.74 × 10^{-5} / 1.99 × 10^{-7} / 3600 = 0.122 s^{-1}.

Considering all Co ions in Co-bipy-900 (451.67 g mol^{-1}) as catalytic centers, M = 451.67/3 = 150.56 g mol^{-1}. $TOF_{theoretical}$ = 10.0 / (4 × 96485 × 0.03 / 150.56) = 0.13 s^{-1} for Co-bipy-900 @GC at 10.0 mA cm^{-2}.

F_{OER} = 0.122 s^{-1} / 0.13 s^{-1} × 100 % = 93.8 %

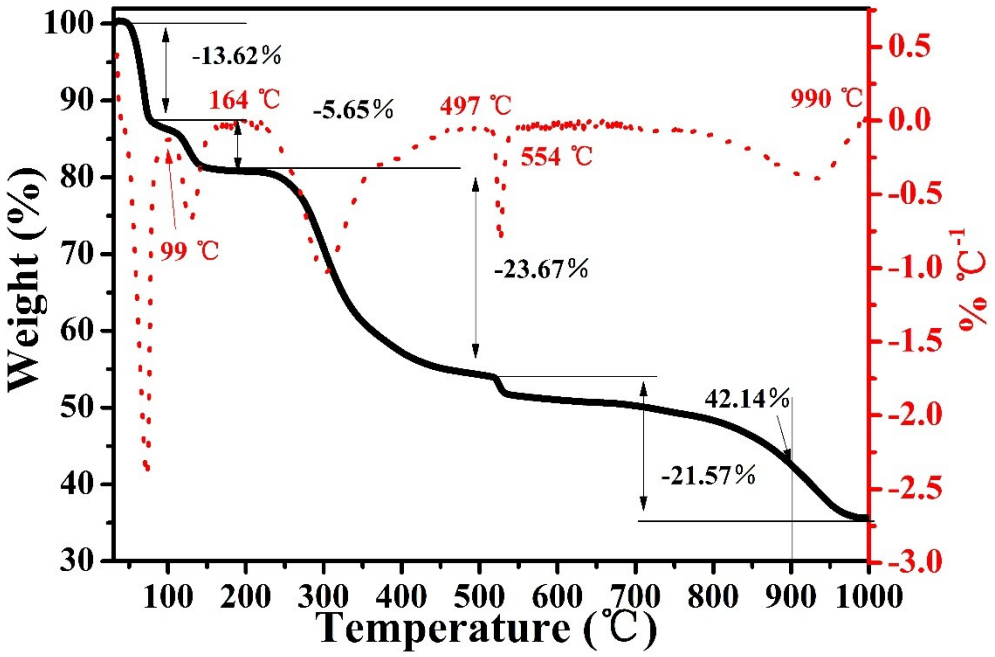

Figure S1. TG curves of Co-Pi-bipy.

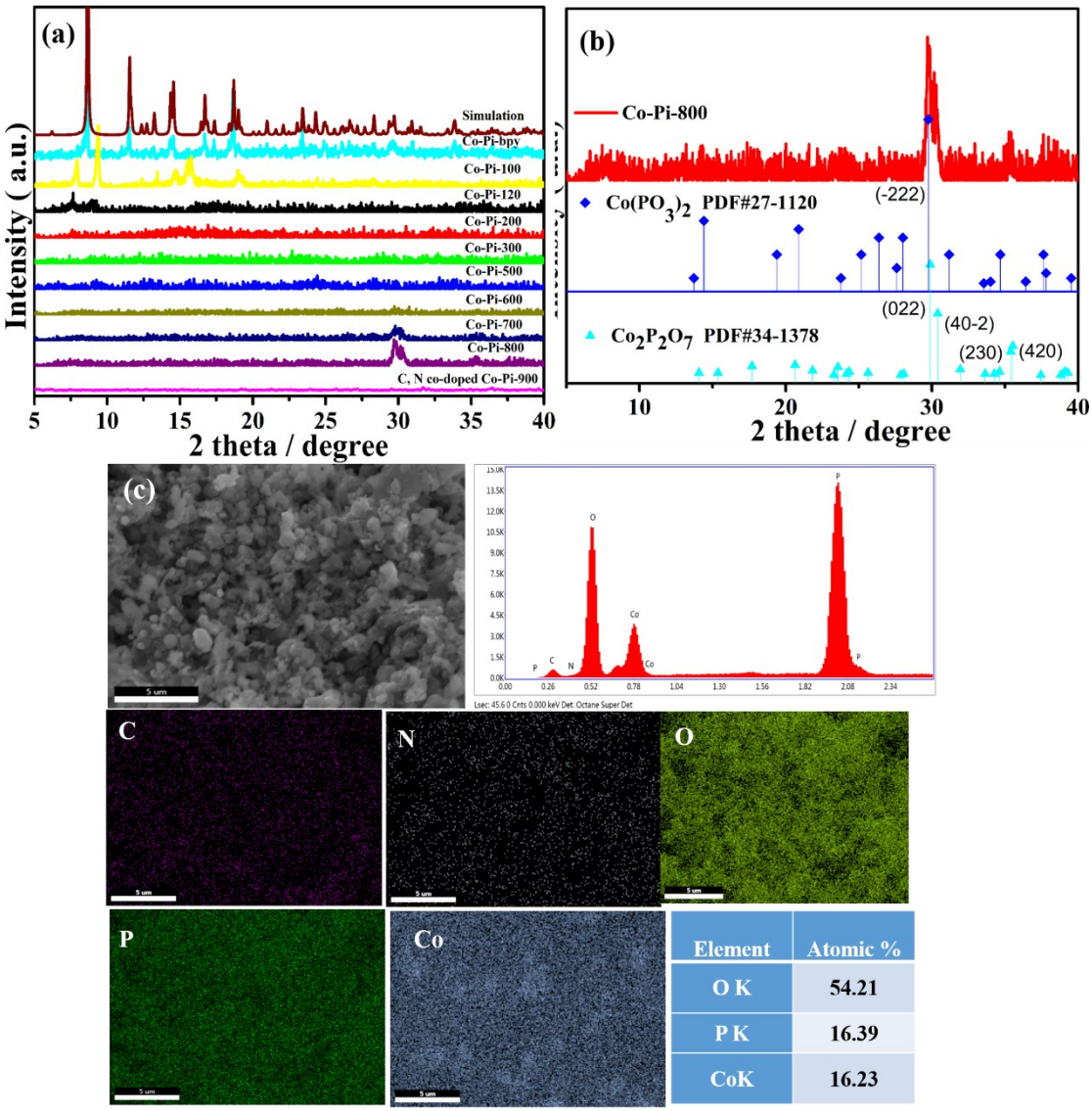

Figure S2. (a)XRD of different product at different TG curves of Co-Pi-bipy, denoted as Co-Pi-T (T= 120, 200, 300, 500, 600, 700, 800℃), Co-Pi-bipy and Co-Pi-900 is C,N co-doped Co-Pi-900), (b) XRD of Co-Pi-800, (c) EDX of Co-Pi-900.

Notes: According to TGA result as shown Figure S1, we can obtain the experimental total weight loss is 57.84% and 64.54% at 900 and 1000°C, respectively, if the final product is a mixture of $Co(PO_3)_2$ and $Co_2P_2O_7$ in a 1:1 molar ratio based on the composition in this MOF precursor, $Co_3(H_2L)_2(H_2O)_4(bipy)_2 \cdot 11H_2O$, the calculated

total weight loss is 60.24%, if the final product is 3.0 mmol $Co(PO_3)_2$, the calculated total weight loss is 49.15%, while the final product is 1.5 mmol $Co_2P_2O_7$, the calculated total weight loss is 65.79%, thus, the experimental total weight loss is closer to that of a mixture of $Co(PO_3)_2$ and $Co_2P_2O_7$. In addition, we also carried out XRD for the calcined sample at different temperature (Figure S2), it can be seen that the new diffraction peaks appear when the sample was heated to 700 °C, the two diffraction peaks at 29.9° and 31.0° could be ascribed to the $(\bar{2}22)$ and $(40\bar{2})$ plane of $Co(PO_3)_2$ and $Co_2P_2O_7$, respectively, as shown in Figure S2b, again suggesting the formation of a mixture of $Co(PO_3)_2$ and $Co_2P_2O_7$. Further, we have measured EDX to investigate the composition of the calcined material (Figure S2c). The EDX analysis of the Co-Pi-900 gave an molar ratio of Co/P/O of ~1.0:1.01:3.34, which is close to that calculated value of a mixture of $Co(PO_3)_2$ and $Co_2P_2O_7$ in a 1:1 molar ratio, and ICP analysis gave Co and P content of 41.16 wt% and 22.98 wt%, respectively, in agreement with EDX results, confirming the elemental composition for the Co-Pi-900. These results indicated that the ccalcined product at 900 °C might be mainly the mixture of $Co(PO_3)_2$ and $Co_2P_2O_7$. We also carried out elemental analysis to find out the percentage of doped carbon and nitrogen for the sample Co-Pi-900, the results indicated that the N and C content of the final product is 0.50%, 7.01%, respectively, confirming the Co-Pi-900 catalyst was a C,N-co incorporated cobalt-based phosphate.

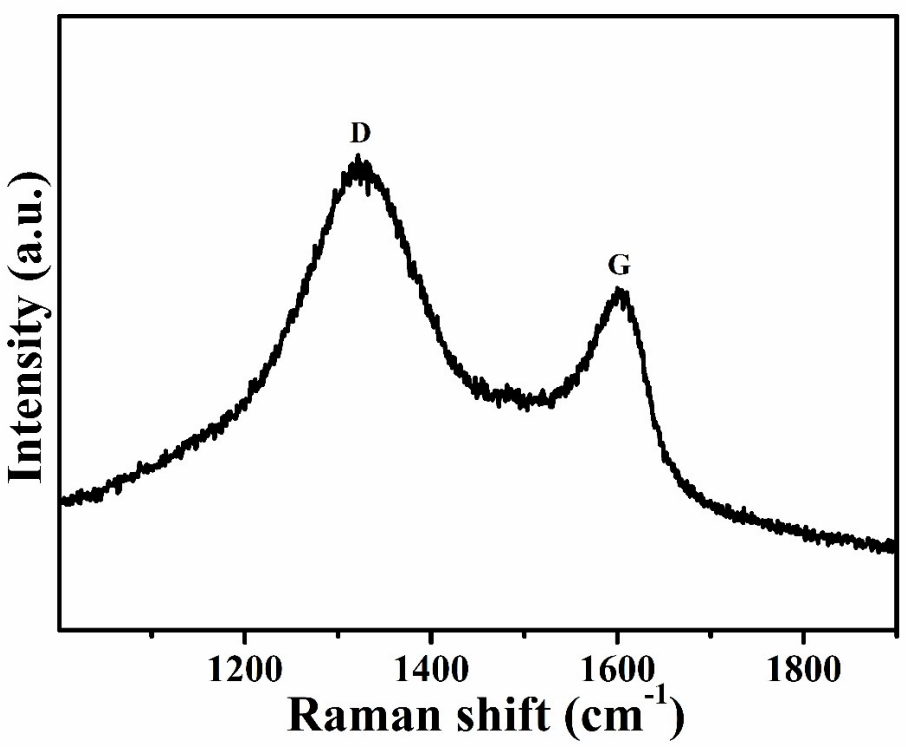

Figure S3. Raman spectrum of compounds Co-Pi-900.

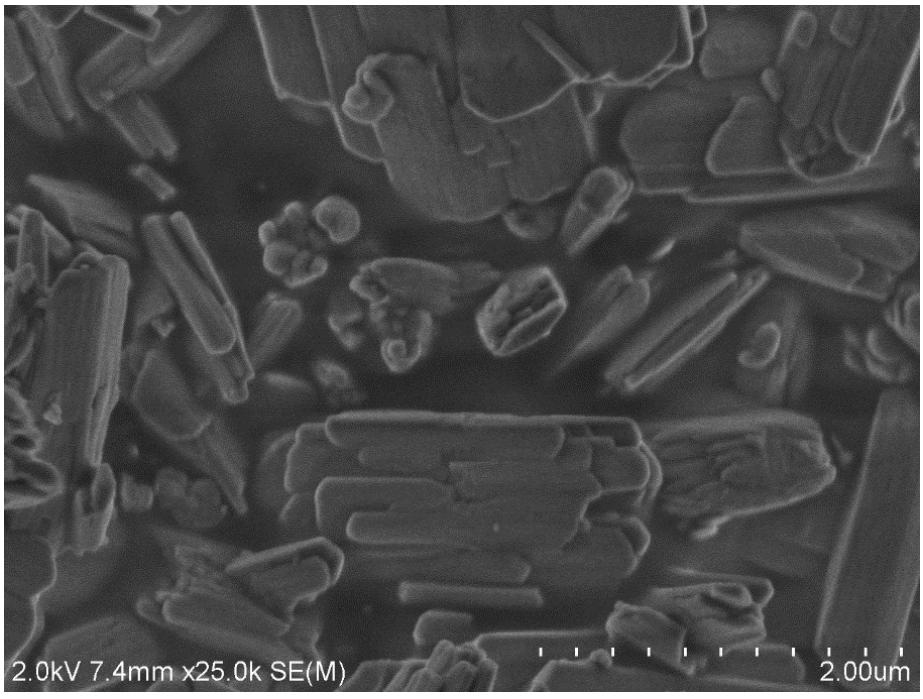

Figure S4. SEM images of Co-Pi-bipy.

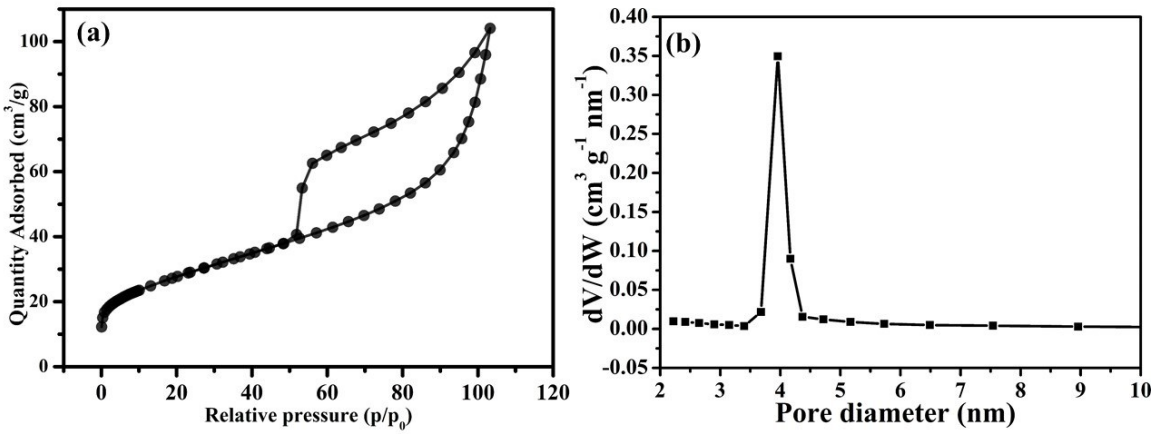

Figure S5. N_2 adsorption (solid) and desorption (open) isotherms (a) and BJH size distribution (b) of C,N co-doped Co-Pi-900, at 77.42 K.

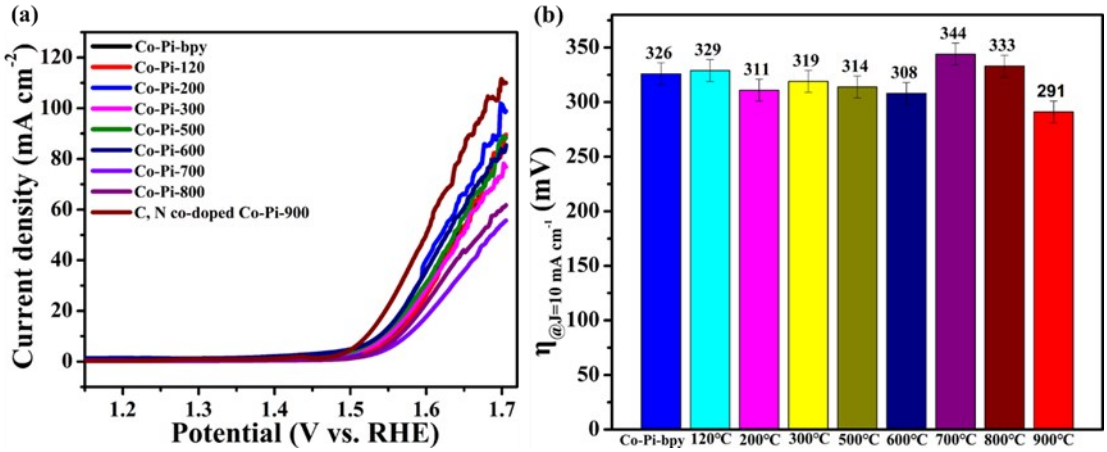

Figure S6. (a) LSV curves of Co-Pi-T (T= 120, 200, 300, 500, 600, 700, 800℃), Co-Pi-bipy and C,N co-doped Co-Pi-900 or Co-Pi-900) at a scan rate of 5 mV/s for the OER, (b) Comparison of the OER overpotential at a current density of 10 mA/cm^2 for Co-Pi-bipy-T catalysts, the error bar represents the range of results from three independent measurements.

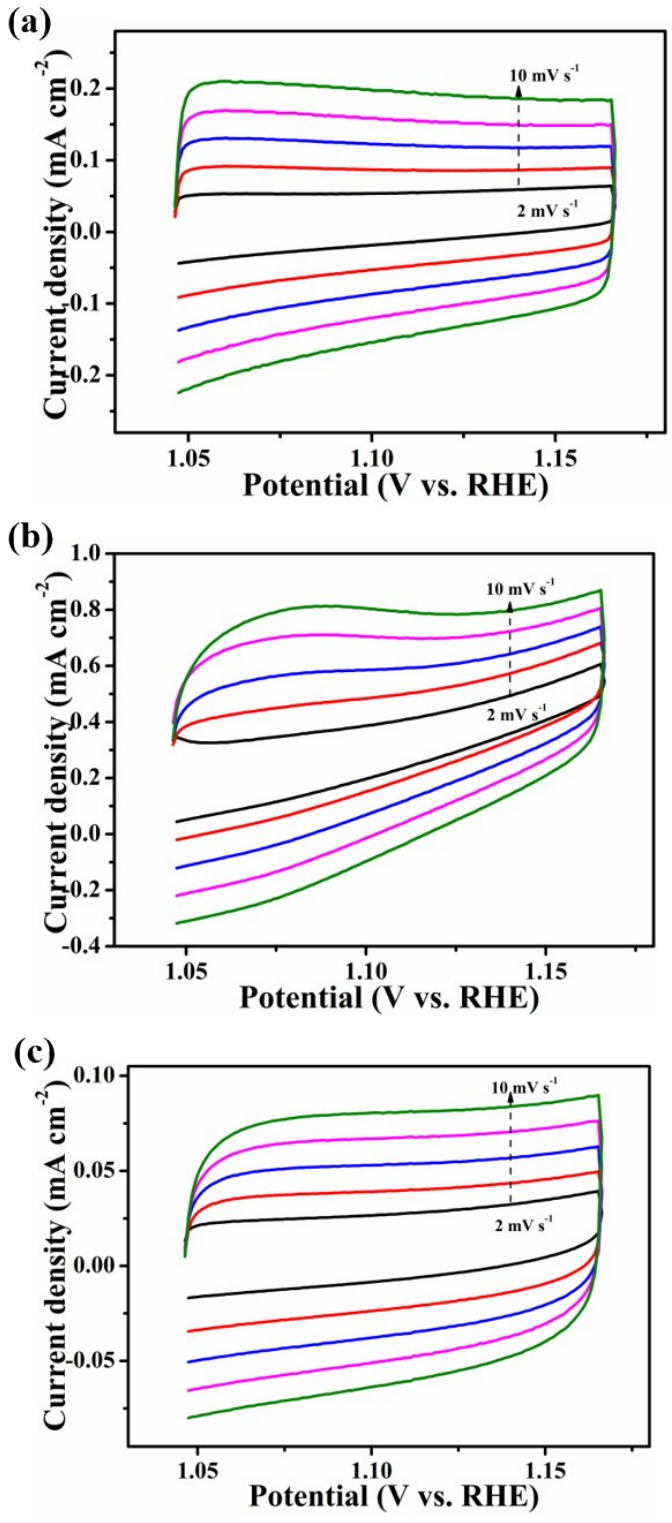

Figure S7. Cyclic voltammograms of (a) Co-Pi-bpy, (b) Co-Pi-900 (C,N co-doped Co-Pi-900) and (c) IrO_2 at different scan rates from 2 to 10 mV s^{-1}.

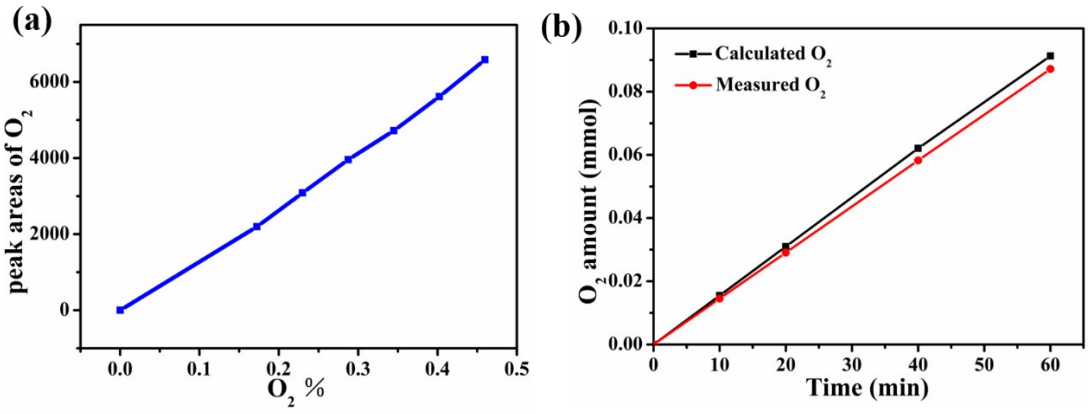

Figure S8. A linear relationship between seven calibrated O_2 concentrations and their gas chromatography peak areas was obtained (a) and the amount of O_2 theoretically calculated and experimentally measured versus time for the OER of Co-Pi-900 (C,N co-doped Co-Pi-900).

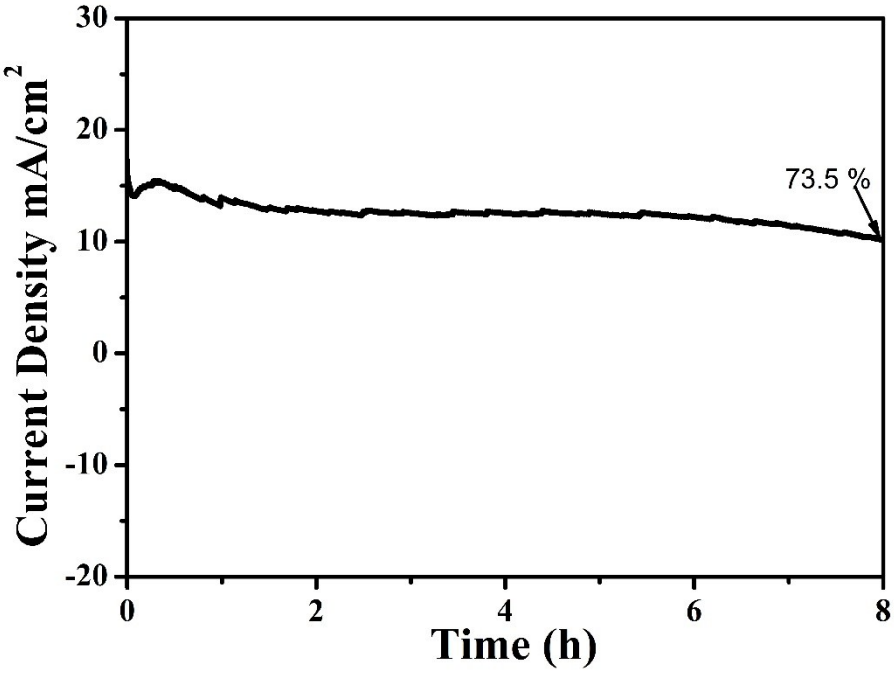

Figure S9. Durability test for the Co-Pi-900 (C,N co-doped Co-Pi-900) sample at 1.56 V (vs. RHE) for 8 hrs.

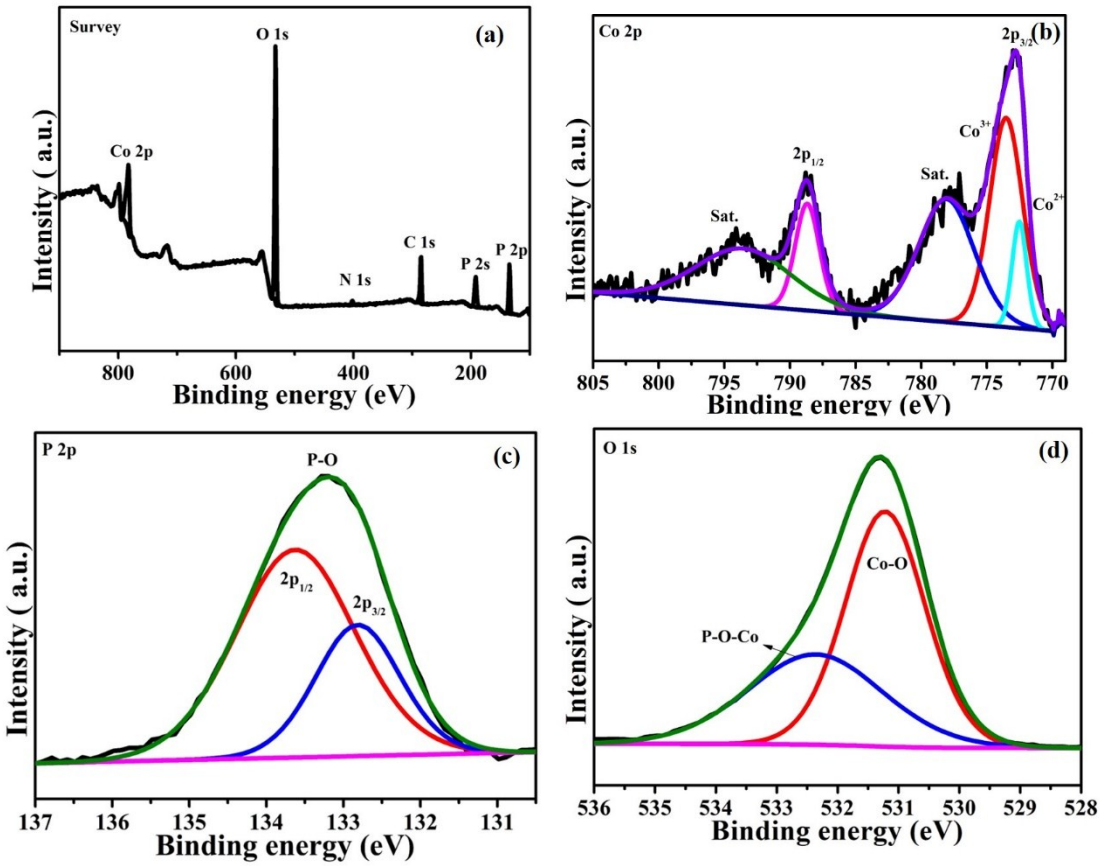

Figure S10. (a)XPS spectrum of Co-Pi-900 (C,N co-doped Co-Pi-900) after OER test in 1.0M KOH, (b) Co 2p, (c) P 2p and (d) O 1s.

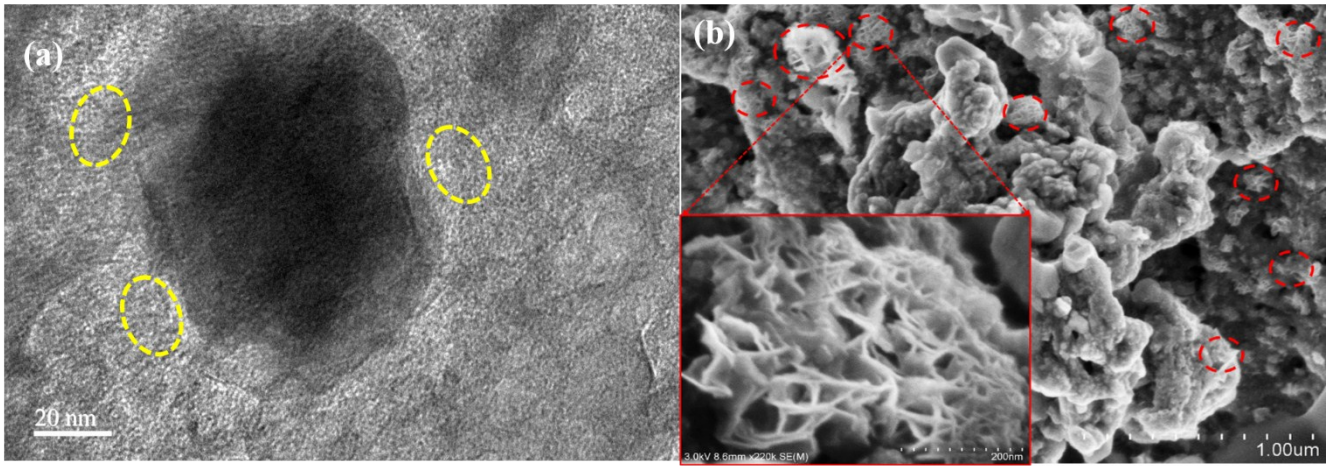

Figure S11. (a) TEM and (b) SEM of Co-Pi-900 (C,N co-doped Co-Pi-900) after OER test in 1.0M, pores and nanosheets are designated as yellow and red circles, respectively.

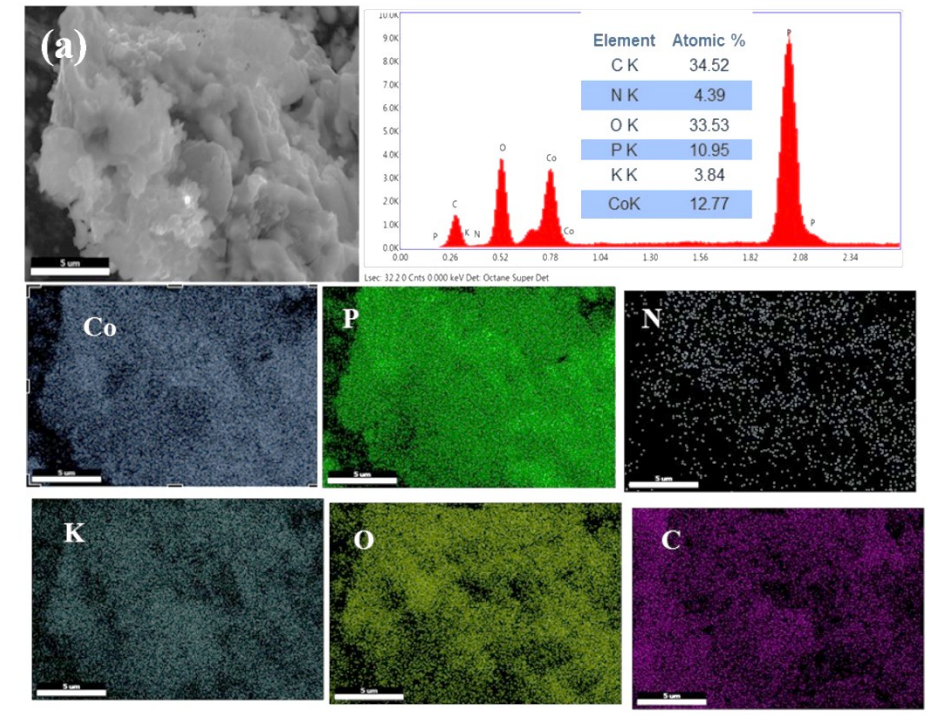
(a)
Element Atomic %
C K 34.52
N K 4.39
O K 33.53
P K 10.95
K K 3.84
CoK 12.77
Co
P
N
K
O
C

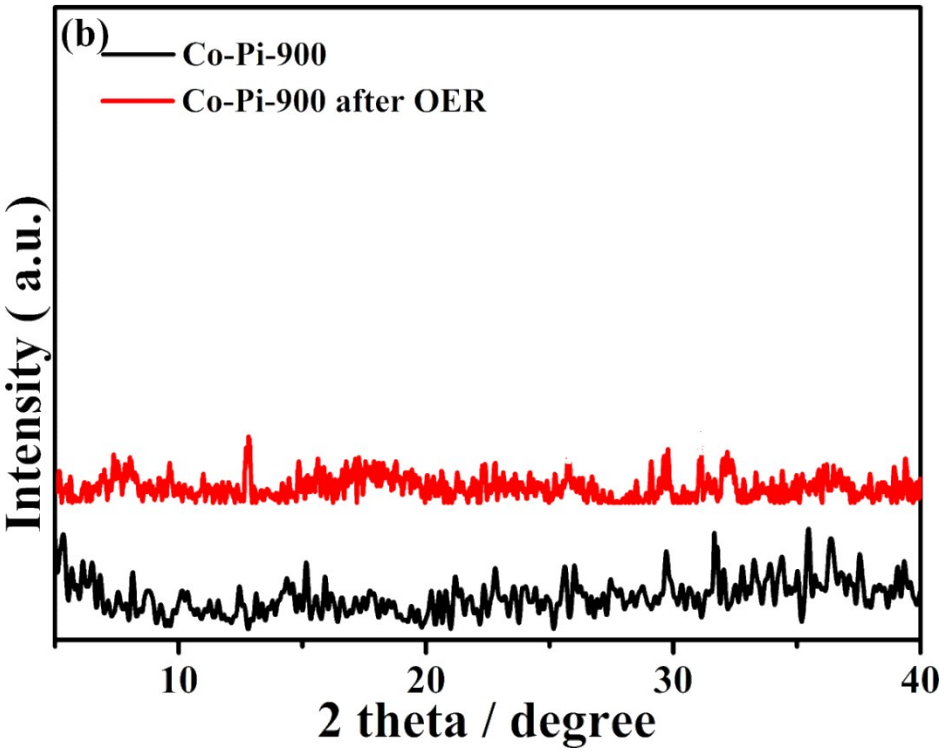
(b)
Co-Pi-900
Co-Pi-900 after OER
Intensity (a.u.)
10
20
30
40
2 theta / degree

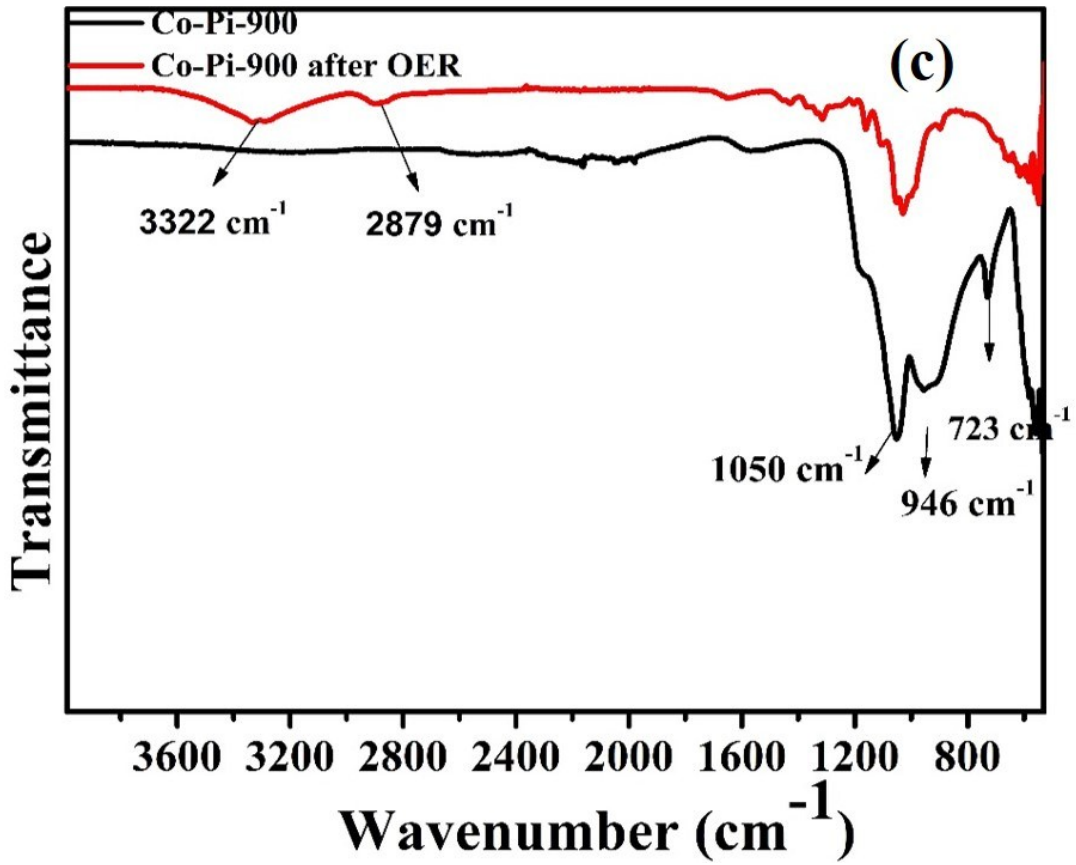

Figure S12. (a) EDX, (b) XRD and (c) FTIR of Co-Pi-900 (C,N co-doped Co-Pi-900) after OER test in 1.0 M KOH.

Notes: The post-catalytic sample after OER test was studied to investigate the surface composition of the catalyst (Figure S10-S12). XPS analysis confirms the existence of Co, P, O, N and C on the surface of the post-catalyst after OER test, in addition, the relative intensity of the O1s peak increases, while, the relative intensity of N1s and P1s decrease, indicating the partial transformation from metal phosphate to hydrated oxides or oxyhydroxides. The Co 2p binding energy for Co ions almost no shifts, and a slight shift to lower binding energy for O 1s is observed, while the P1s showed a slight shift to higher binding energy, which might be attributed to the formation of hydrated oxides or oxyhydroxides in the surface of amorphous post-catalyst after the

OER test. Pores also could be clearly observed in TEM micrographs of the sample (light areas marked as res circles on Figure S11a). The SEM of the post-catalytic sample after OER test (Figure S11b) shows that the sample displayed slight aggregation compared with that of pristine catalyst, in addition, the nanosheets after OER test are slightly rougher than that of the catalyst before OER test. The FTIR spectra of Co-Pi-900 and Co-Pi-900 after OER test were shown in Figure S11c. The characteristic peak at 1050 cm^{-1} for both samples corresponds to characteristic vibration of phosphate groups. The new broad vibration peak at 3322 cm^{-1} and 2879 cm^{-1} indicate the appearance of adsorbed OH^- groups in the post-catalyst. EDX analysis (Figure S12a) exhibits the regular distribution of Co, P, O, N and C, notably, only small amount of N and C the surface of the catalyst, and compared with EDX of the pristine sample, the molar ratio of Co/P/O of the post-catalytic sample is 1.0:0.85:1.12, indicating the partial loss of P atoms, in accordance with XPS and FTIR results. The XRD pattern after OER test shows still no diffraction peaks, suggesting it was still amorphous structure. Combining these results, the electrocatalyst after OER test has been partially transformed into hydrated oxides or oxyhydroxides in 1.0 KOH, the active material on the surface of Co-Pi-900 possibly was mainly the mixture of cobalt hydroxide and cobalt phosphate.

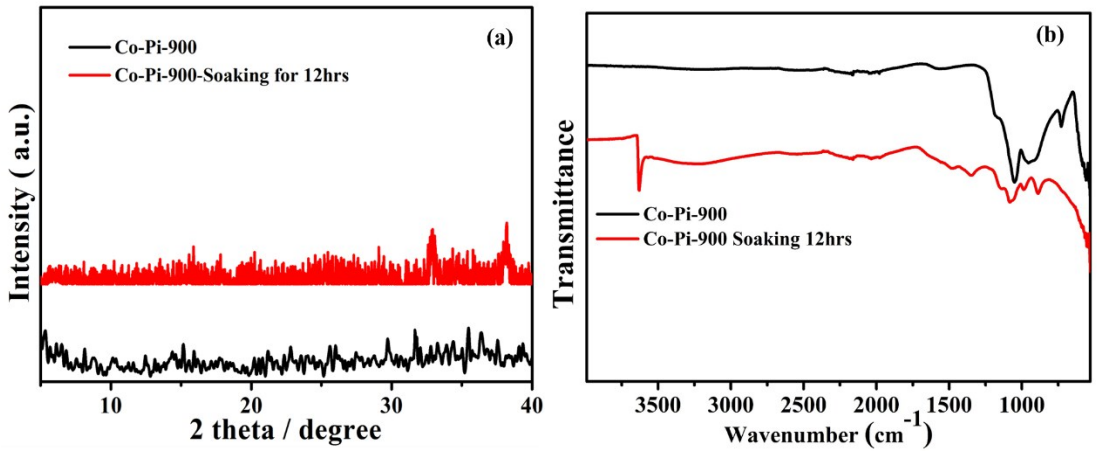

Figure S13. (a) XRD, (b) FTIR of Co-Pi-900 and Co-Pi-900 (C,N co-doped Co-Pi-900) soaking for 12hrs.

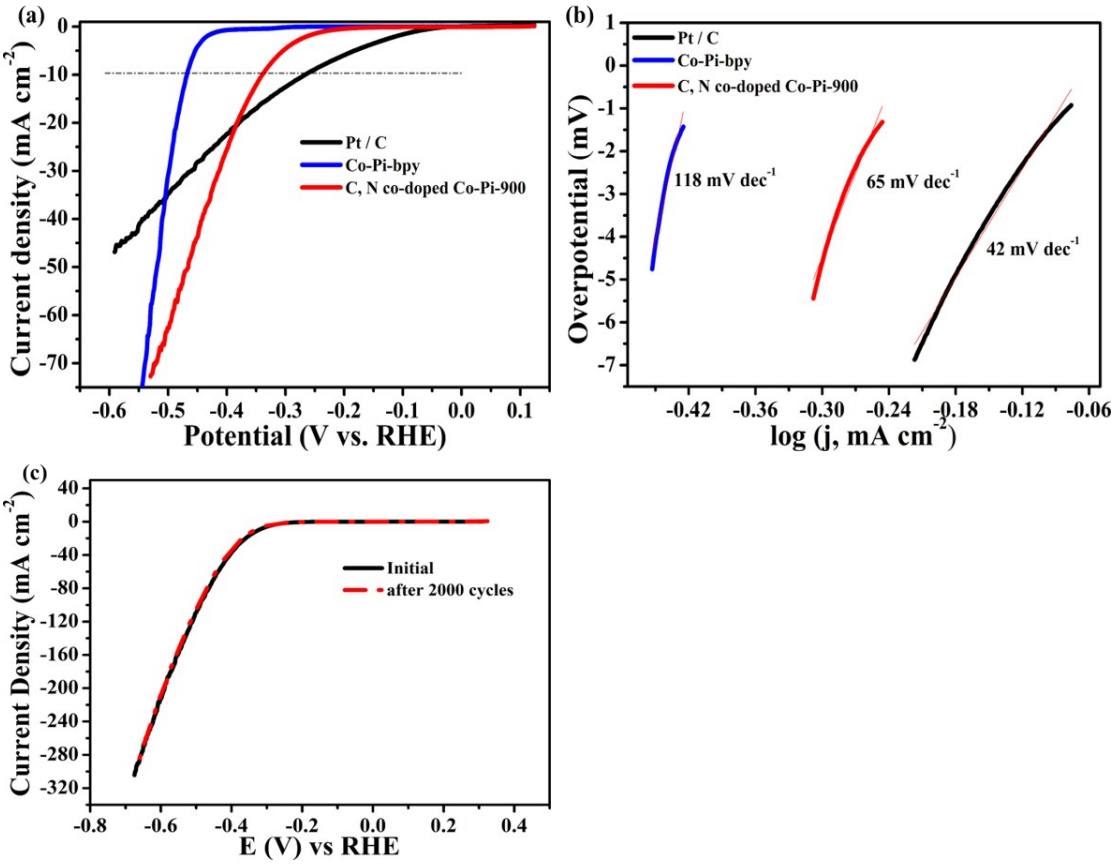

Figure S14. (a) HER polarization curve of Co-Pi-900 (C,N co-doped Co-Pi-900), sweep rate: 5 mV s^{-1} in 1 M KOH. Pt/C, Co-Pi-bpy are also added for comparison. (b) Corresponding Tafel plots of the samples shown in (a). (c) Durability test for the Co-Pi-900 (C,N co-doped Co-Pi-900) sample. Pt/C (commercial Pt/C, 5% Pt) was compared as a reference.

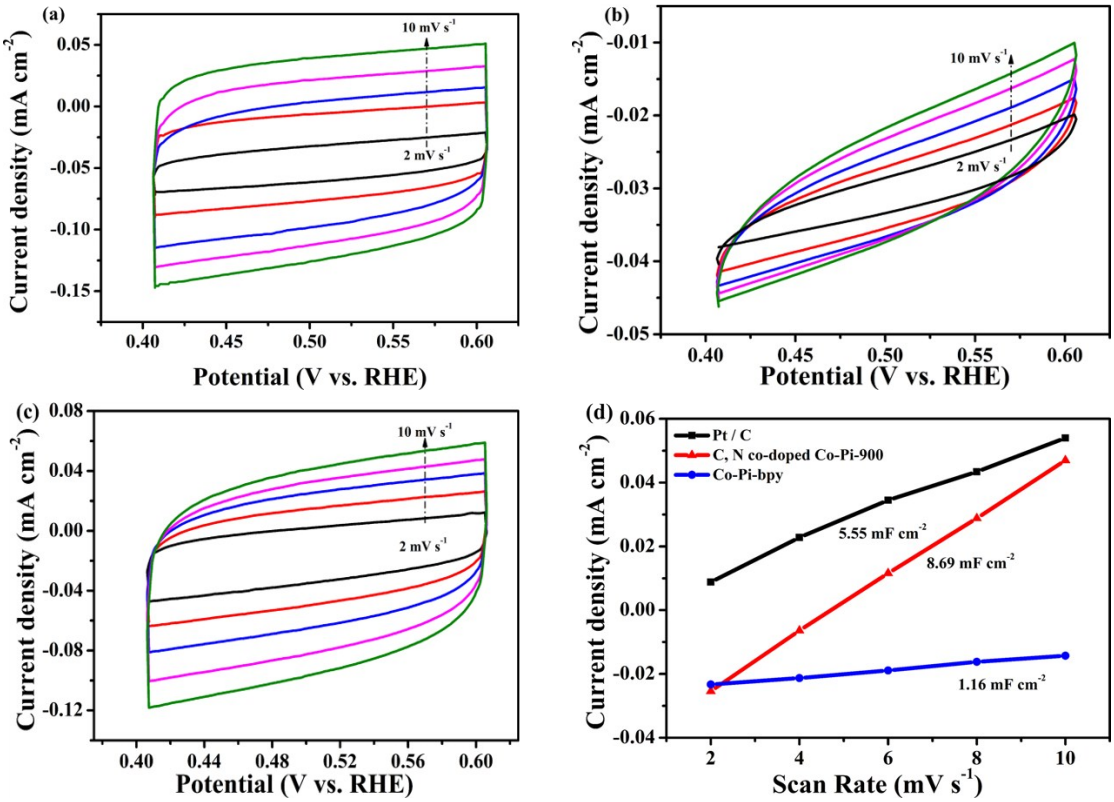

Figure S15. Cyclic voltammograms of (a) Co-Pi-900 (C,N co-doped Co-Pi-900), (b) Co-Pi-bpy, (c) IrO_2 at different scan rates from 2 to 10 mV s^{-1}. (d) Plots of the current density at 0.57 V vs. the scan rate for different catalyst. All experiments were carried out in 1.0 M KOH.

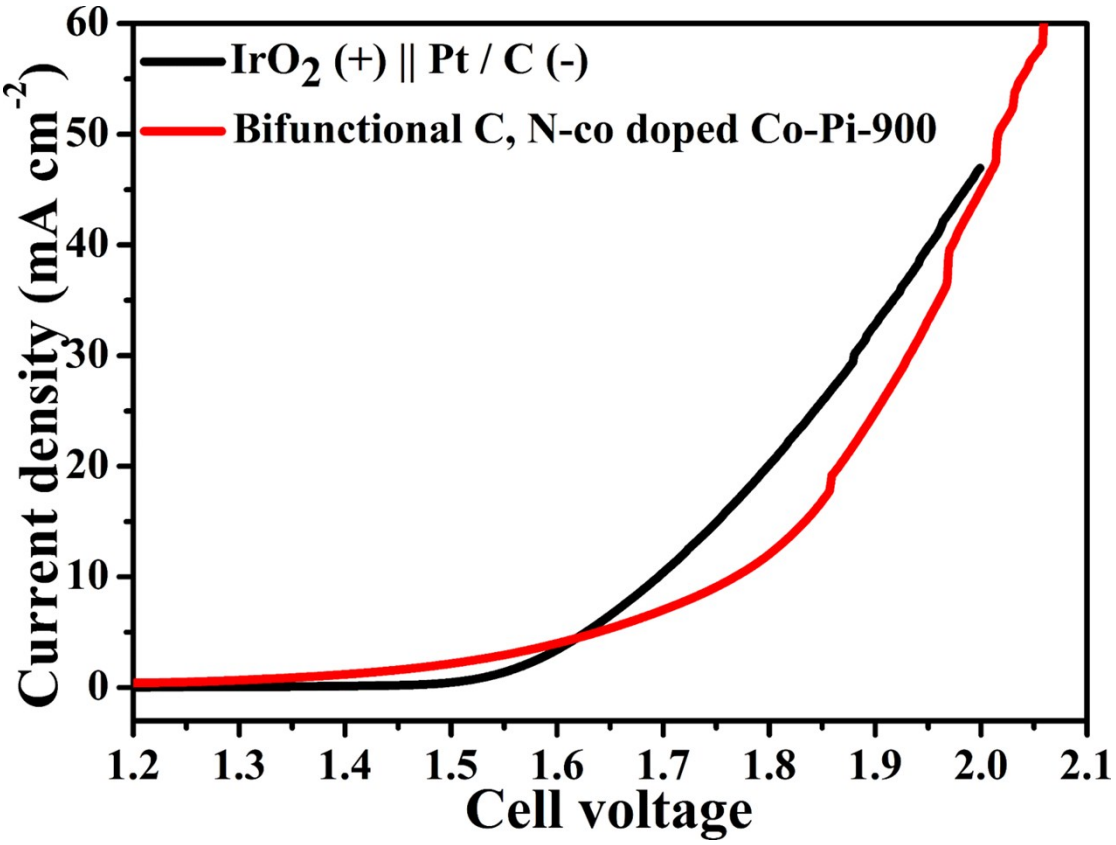

Figure S16. (a) Polarization curve for overall water splitting with the Co-Pi-900 (C,N co-doped Co-Pi-900) electrode as both the anode and cathode.